Dicle University
Journal of Engineering
https://dergipark.org.tr/tr/pub/dumf
duje.dicle.edu.tr

Research Paper

Numerical Investigation on Hydrogen-Blended Methane Combustion in a MILD Combustor

Mustafa Kemalettin BÜYÜKAKIN[1*]

[1]Trakya University, Mechanical Engineering Department, mkbuyukakin@trakya.edu.tr, Orcid No: 0000-0002-0791-0651

ARTICLE INFO

Article history:

Received 16 April 2026
Received in revised form 13 July 2026
Accepted 16 July 2026
Available online 8 August 2026

Keywords:

MILD combustion, hydrogen fuel, combustion mode

Doi: 10.24012/dumf.1930501

* Corresponding author

ABSTRACT

This study numerically investigates the combustion characteristics of pure methane and hydrogen-blended methane in a MILD (moderate or intense low-oxygen dilution) combustor. Three different combustion models, namely the chemical equilibrium, steady diffusion flamelet and eddy dissipation concept, were employed with the use of ANSYS Fluent 18.1 software. The chemical equilibrium and steady diffusion flamelet models failed to agree with the experimental data of the pure methane case, while the eddy dissipation concept model showed the best agreement with the experimental data. Two different sets of the hydrogen addition studies were conducted in the simulations under the constant thermal load and constant methane consumption conditions. The hydrogen addition ratio to methane was varied from 10% to 40% on molar basis. The obtained results reveal that the hydrogen addition makes the combustion flame more compact and increases the reaction rate of methane, which in turn reduces the MILD combustion characteristics of the combustor.

Introduction

There are mainly two different combustion modes in the field of combustion science and engineering. The first one is the conventional mode or fast chemistry mode, in which the reaction rate of a fuel can be assumed to be infinitely fast by being a function of turbulence. In other words, the combustion is dictated by turbulent mixing in flow field. This combustion mode is well established in many practical systems such as industrial or domestic boilers, furnaces and combustion engines. The other one is the MILD combustion mode, which occurs under diluted oxygen conditions. The reaction rates of fuel species are lowered in this regime and become comparable with turbulent time scales. In addition, the flame temperature drops and its volume becomes expanded due to distributed fuel reaction. The dilution of oxidizer can be managed by internal recirculation of combustion products or mixing of inert gases into air prior to entering combustion volume. If internal recirculation is to be utilised in order to sustain the MILD combustion conditions, the process becomes dependent on combustion volume configuration. The latter requires pre-heating of the oxidizer air in order to sustain the reactions in the flow field [1]. According to Cavaliere and de Joannon [1], a combustion process is MILD if the inlet temperature of reactants is higher than the self-ignition temperature, while the maximum temperature increase from the inlet condition is lower than the self-ignition temperature. Luan et al. [2] stated that a critical oxygen molar fraction under the diluted conditions is needed to sustain the MILD combustion with temperature of reactants being higher than the self-ignition temperature. The benefits of the MILD combustion are that the combustion flame is expanded, which can increase thermal efficiency while lowering the NO_X emissions due to decreased flame temperature level. The disadvantages can be the restricted operating conditions as given on the inlet temperature-temperature increase chart of Cavaliere and de Joannon [1] and the exhaust gas recirculation-furnace temperature chart of Wünning and Wünning [3]. The combustion instabilities can stem from these restricted operating conditions of the MILD mode.

Natural gas or pure methane is the lightest hydrocarbon, which is commonly used in all the industrial and domestic sectors. Many research and engineering studies employing MILD or conventional combustion modes exist on the efficient utilisation of natural gas together with other hydrocarbons. Hydrogen or ammonia (a hydrogen carrier) addition to hydrocarbon fuels on the other hand is one of the techniques to alter the combustion mode and efficiency.

Hydrogen has distinct different physical and chemical properties compared to natural gas. Hydrogen has considerably lower density and wide flammability range, which also shortens the ignition time [4]. It is highly reactive and forms heat and active radicals needed in the combustion environment [5]. These features of hydrogen and its carbon-reducing effects make it very plausible to utilise and alter the combustion flame mode and emissions of hydrocarbon fuels.

Some of the research studies conducted on the MILD combustion and hydrogen-blending are briefly reviewed. Rebola et al. [6] studied experimentally on methane MILD combustion in a small-scale burner. They investigated the effects of the thermal input, excess air coefficient, reactant temperature and velocity on the combustor performance. The wall temperature effect on the temperature uniformity and species were revealed in this study. It was determined that the configuration parameter to sustain the MILD combustion was the bottom end part of the combustor having a convergent nozzle at an angle of 35º, which contributed to the recirculation of the combustion products into the flame. Fordoei et al. [7] studied numerically on the MILD combustion of methane fuel by diluting the combustion air. The dilution ratio was up to 90% by CO_2. The authors also examined on the chemical and physical effects of the diluents. They concluded that the dilution of the combustion air made the CH_2O species more distributed in the combustor as an indicator to improve the MILD combustion behaviour. Rebola et al. [8] studied numerically to investigate the performance of the various turbulence models and combustion models for MILD combustion. The authors utilised the experimental data of their previous study [6]. They concluded that EDC model performed the best for the prediction accuracy, while the choice of the turbulence models did not influence the predictions considerably. Rashed et al. [9] conducted some series of the numerical studies on NH_3/H_2 fuel combustion under the MILD conditions. The authors showed that the hydrogen enrichment made the flame more reactive and the flame was shifted upstream towards the burner inlet. The flame switched to the conditional-MILD mode from the unconditional-MILD mode up to the enrichment ratio of 40% on molar basis. Xu et al. [10] stated in their numerical study that hydrogen addition to methane diminished the MILD mode of the combustion flame. The authors also resulted that Damköhler number increased with hydrogen addition. Zourazmai et al. [11] studied numerically on a MILD combustor by altering the bluff body design of the combustor to a linear configuration. The authors determined that the linear configuration angle of 15° performed the best to obtain the temperature uniformity and to increase the mixing rate of the reactants. Jowkar et al. [12] analysed numerically ammonia spray combustion under the diluted conditions. The authors showed that the dilution of the oxidizer made the flame more distributed in the combustor. In addition, increasing the inlet temperature of the diluted oxidizer formed more localised flame zones resulting in more intense heat release rates. Mardani et al. [13] investigated experimentally an ammonia-hydrogen-methane combustor under the pre-heated and diluted air conditions. Their results showed that the chemiluminescence level of the flame decreased under the pre-heated and diluted conditions compared to the normal air case. In addition, it was stated that hydrogen addition to ammonia for the normal air condition lowered the lean blow out level compared to the methane-ammonia blending cases. This was attributed to the higher reactivity of hydrogen fuel. Büyükakın [14] numerically examined the hydrogen-enriched methane combustion up to 40% addition ratio under the moderately diluted air conditions. It was deduced that the hydrogen enrichment improved the methane combustion stability and shifted the flame from the distributed mode to the conventional mode.

MILD combustion is a complex process, which integrates interlinked chemical and turbulence aspect in the flow field. In addition, the research studies in the available literature show that it is highly case dependent. On the other hand, hydrogen enrichment of hydrocarbon fuels is becoming increasingly common to reduce carbon emissions and enhance flame behaviour in combustors. It is deduced that both MILD combustion and hydrogen enrichment focus on cleaner and more efficient combustion processes and need more addressing in the current literature. This paper numerically contributes to the literature on the thermal uniformity, reactant mixing and fuel reactivity effects of hydrogen enrichment of methane. A MILD combustor, which relies on the recirculation of the combustion products is employed. EDC combustion model is utilised for the hydrogen enrichment cases. The effects of the hydrogen enrichment on the combustion parameters are investigated for the constant thermal load and constant methane fuel consumption scenarios. The obtained results are scrutinized in detail.

Methodology

Combustor description

The MILD combustor of the University of Lisbon [6,8] was employed in this numerical study. This combustor measures 150 mm in diameter and 300 mm in length. The burner is located at the top of the combustor. The burner has a central fuel injector with an inner diameter of 4 mm and an outer diameter of 6 mm. The fuel injector is surrounded by the air inlet having an outer diameter of 15 mm. The combustion products are exhausted from a convergent nozzle. This nozzle has a length of 50 mm and 35° angle. The combustor has a straight tube exit, which is located downstream of the convergent nozzle, with a diameter of 85 mm and 150 mm length. The combustor was modelled axisymmetric in 2D and it is presented schematically in Fig.1.

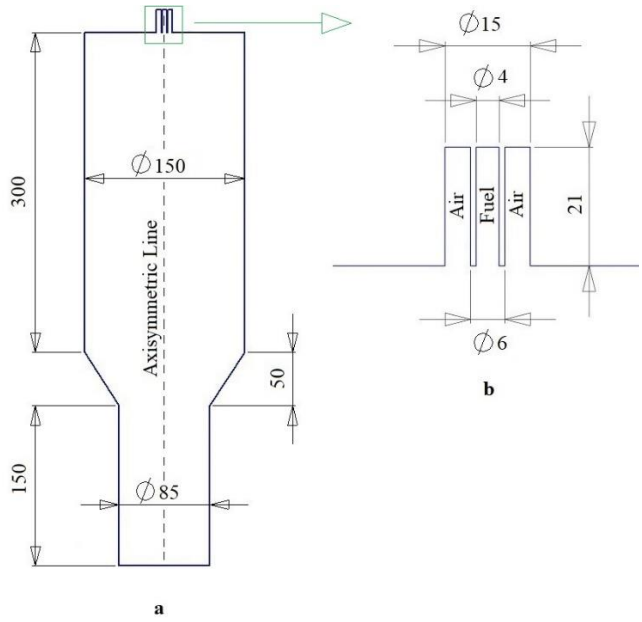

Figure 1. MILD combustor (a) and Burner Inlets (b)

Mathematical modelling

Three main governing equations were solved for the numerical simulations. The mass, momentum and energy equations are given in Eqs. (1-3), respectively [15].

$$\frac{\partial(\rho)}{\partial t} + \nabla.(\rho \mathbf{v}) = 0 \quad (1)$$

$$\frac{\partial(\rho \mathbf{v})}{\partial t} + \nabla.\rho\mathbf{v}\mathbf{v} = -\nabla.\mathbf{P} + \rho \sum_{i=1}^{N} Y_i \mathbf{f_i} \quad (2)$$

$$\frac{\partial(\rho \mathbf{h})}{\partial t} + \nabla.[\rho \mathbf{v} h - \rho D \nabla h + k_L \left(\frac{1}{Le} - 1\right) \nabla T\ ] = S_h \quad (3)$$

The Reynolds-averaging method was considered in this study. The k-ε model [16] was selected for the turbulence modelling as an efficient and time saving model. The standard k-ε model was preferred over the realizable and RNG k-ε models since it predicted the results more accurately. The radiation intensity equation [16] was also solved to calculate the radiative heat transfer of hot gases in the flame. Three different combustion models were utilised in the simulations. These were the chemical equilibrium model, steady diffusion flamelet model (SDFM) and eddy dissipation concept (EDC) model. The mean mixture fraction conservation equation [16] given in Eq. (4) was solved for the chemical equilibrium model and SDFM. It should be noted that Le number in Eq. (3) is taken unity for the chemical equilibrium model and SDFM.

$$\frac{\partial(\rho \bar{f})}{\partial t} + \nabla.(\rho \mathbf{v} \bar{f}) = \nabla.[\left(\frac{k_L}{c_p} + \frac{\mu_t}{\sigma_t}\right) \nabla \bar{f}\ ] \quad (4)$$

The mean scalar values were calculated for the chemical equilibrium model and SDFM as given in Eq. (5) and Eq. (6), respectively [16]. The scalar term ∅ in Eq. (6) was obtained from the flamelet equations [16]. DRM19 reaction mechanism [17] was utilised in the flamelet equations. The chemistry-turbulence interaction was taken into account with the probability density function (PDF) [16]. PDF is designated as P_f and P_χ in Eq. (5) and Eq. (6). It should be noted that Eq. (6) is written for adiabatic flamelets, while the mean enthalpy level $\bar{H}$ is also taken into account for the calculation of the mean temperature and density in the non-adiabatic SDFM. Since PDF is also a function of $\overline{f'^2}$ (mean mixture fraction variance), a conservation equation for $\overline{f'^2}$ [16] was also solved in the calculations.

$$\bar{\emptyset} = \int_0^1 \emptyset(f, \bar{H}) P_f(f)\, df \quad (5)$$

$$\bar{\emptyset} = \iint \emptyset(f, \chi_{st}) P_f(f)\, P_\chi(\chi_{st}) df\, d\chi_{st} \quad (6)$$

A transport equation for the mean value of each species in the reacting flow was solved when EDC model was employed. This equation is given in Eq. (7) [16]. The diffusion flux term is given in Eq. (8) employing the default constant molecular diffusion coefficient given in the software. DRM19 reaction mechanism [17] was employed for the finite-rate reactions of the chemical species. The finite-rate reactions in the reaction mechanism are assumed to take place in the fine-scale structures where turbulence kinetic energy dissipates into heat and molecular mixing occurs.

$$\frac{\partial(\rho \bar{Y}_i)}{\partial t} + \nabla.(\rho \mathbf{v} \bar{Y}_i) = -\nabla.J_i + \bar{R}_i \quad (7)$$

$$J_i = -\left(\rho D + \frac{\mu_t}{Sc_t}\right) \nabla \bar{Y}_i \quad (8)$$

$\bar{R}_i$ in Eq. (7) is the mean reaction rate of the i_{th} species and it is modelled as given in Eq. (9) [16]. In this equation, τ^*, ξ^*, and Y_i^* are respectively time scale (s), length fraction of fine scales and fine-scale mass fraction of the i_{th} species after the reactions occur.

$$\bar{R}_i = \frac{\rho \xi^{*2}}{\tau^*[1-\xi^{*3}]} (Y_i^* - \bar{Y}_i) \quad (9)$$

It should be noted that when the chemical equilibrium model and SDFM were employed, Eq. (5) and Eq. (6) were solved by the software prior to the simulations and the results were tabulated. The steady state conditions were considered in the simulations. The coupled scheme was used for pressure-velocity coupling. The second order upwind scheme was used for the discretization of the equations, while the second order was selected for the pressure. The least squares cell based was selected for the gradient. The discrete ordinates model (DO) was utilised for the radiation modelling and the WSGGM-domain based [16] was used for the absorption coefficient. The velocity inlet boundary condition was assigned to the inlets and the atmospheric pressure condition was assigned to the outlet. The convergence limit was 10^{-6} for all the equations, as it was 10^{-5} for the continuity equation. In addition, the mean temperature along the central line of the combustor and the energy balance of the fluid volume were monitored during the simulations. The constant central temperature value and

the near-zero net energy flux into the fluid domain were ensured for the convergence.

Meshing studies and validation

The mesh independence study was performed by changing the mesh element size between 0.45 mm and 1 mm. These element sizes were used for the whole fluid zone, since this study investigated the MILD or distributed combustion behaviour of the different fuel mixtures. The quad mesh elements were used in the fluid zone. Table 1 presents the different tested mesh element sizes and numbers in this study. The experimental study conditions of Rebola et al. [6] were employed for the mesh independence studies. The parameters of the experimental study of these authors are given in Table 2.

Table 1. Meshing Parameters

Case	Element Size	Element Number
Meshing 1	1 mm	32029
Meshing 2	0.8 mm	49934
Meshing 3	0.6 mm	86683
Meshing 4	0.5 mm	126934
Meshing 5	0.45 mm	157870

Table 2. Experimental Operating Conditions

Methane inlet velocity 38.1 m/s	**Air inlet velocity** 155 m/s
Fuel inlet temperature 20℃	**Air inlet temperature** 700℃
Thermal load 15.6 kW	**Wall temperature** 984℃

EDC model was selected for the meshing studies. The parameter to follow was the temperature variation along the centre of the MILD combustor. The obtained results from the different mesh element sizes are given in Fig.2. It is presented in Fig.2 that the calculated temperature values from the meshing cases with 0.5 mm and 0.45 mm element sizes are very close. Moreover, the maximum deviation in the temperature at any point in the flame zone was around 2% between these two cases. Therefore, the meshing element size was selected as 0.5 mm for the rest of this study.

The numerical results and the experimental data for the operating conditions in Table 2 are compared in Fig. 3 and Fig. 4. It should be noted that the calculated results and the experimental data in Fig. 3 are given along the combustor centreline. It can be deduced from Fig.3 that the chemical equilibrium model and SDFM fail to predict the experimental data for the temperature, CO_2 and O_2 along the combustor centre. This means that the reaction rates in the combustor are influenced by the finite-rate kinetics, making their time scales comparable to turbulence time scales. In this case, the reaction rate of any species is not entirely a function of the turbulent mixing. The dilution and temperature level of the reactants are also dominant in the course of process. EDC combustion model, which takes into account the finite-rate reactions in the fine scales of turbulent flow, performs the best to conform the experimental data. This is another indication that proves the reaction rates are influenced by the reaction kinetics or the combustion is in the MILD mode. It is seen in Fig.3 that EDC model captures the general variation trends of the temperature, CO_2 and O_2 species volume fractions on dry basis. EDC model under predicts the temperature and CO_2 emissions in the vicinity of the burner. This is mainly due to the under prediction of the mixing rate of the hot combustion products and the reactants in the burner inlet zone. The hot combustion products are recirculated by the convergent nozzle to the upstream of the combustor, which helps the dilution of the reactants and the combustion occur in the MILD form. The recirculation rate is thought to be predicted at a low rate around the burner inlet zone due to the limitations in the turbulence modelling and its interaction with the combustion model. This is the reason as to why the temperature and CO_2 emissions are predicted at a low rate, as given in Fig.3, while the O_2 level is calculated higher in the vicinity of the burner compared to the experimental data. The use of LES turbulence model [16] and more advanced EDC models can improve the prediction capability of the simulations. Fig.4 presents the radial distribution of the flame temperature at several axial distances obtained from the numerical calculations and the experimental data. Although there can be seen some deviations from the experimental data due to the limitations of the turbulence and combustion modelling, it is deduced that EDC model performs the best to predict the general trend in the variation of the experimental data. Therefore, this study continued by examining of the hydrogen enrichment effects on the MILD combustion mode of methane fuel with the use of EDC model.

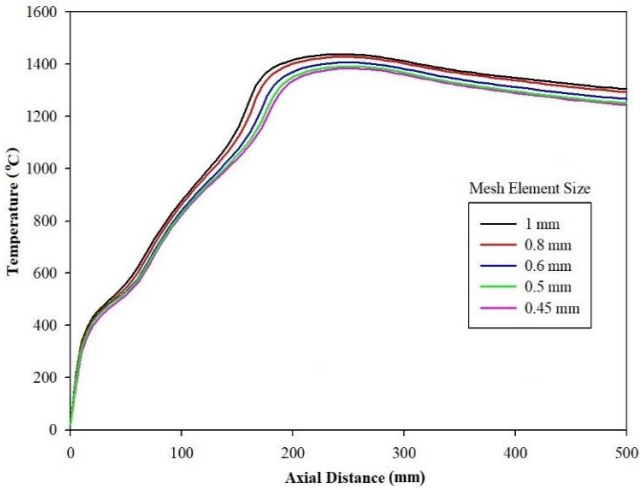

Figure 2. Temperature along Combustor Centre for Different Mesh Element Sizes

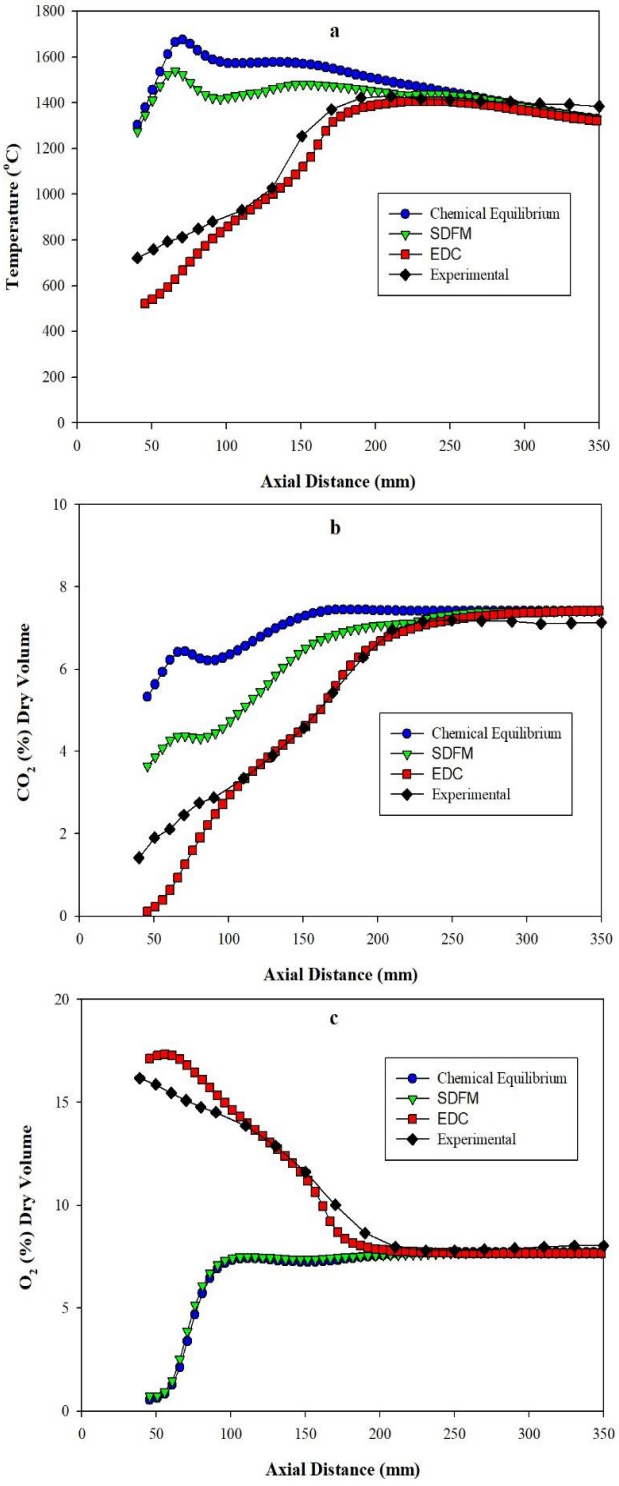

Figure 3. Comparison of Temperature (a), CO_2 (b) and O_2 (c) along the Combustor Centreline

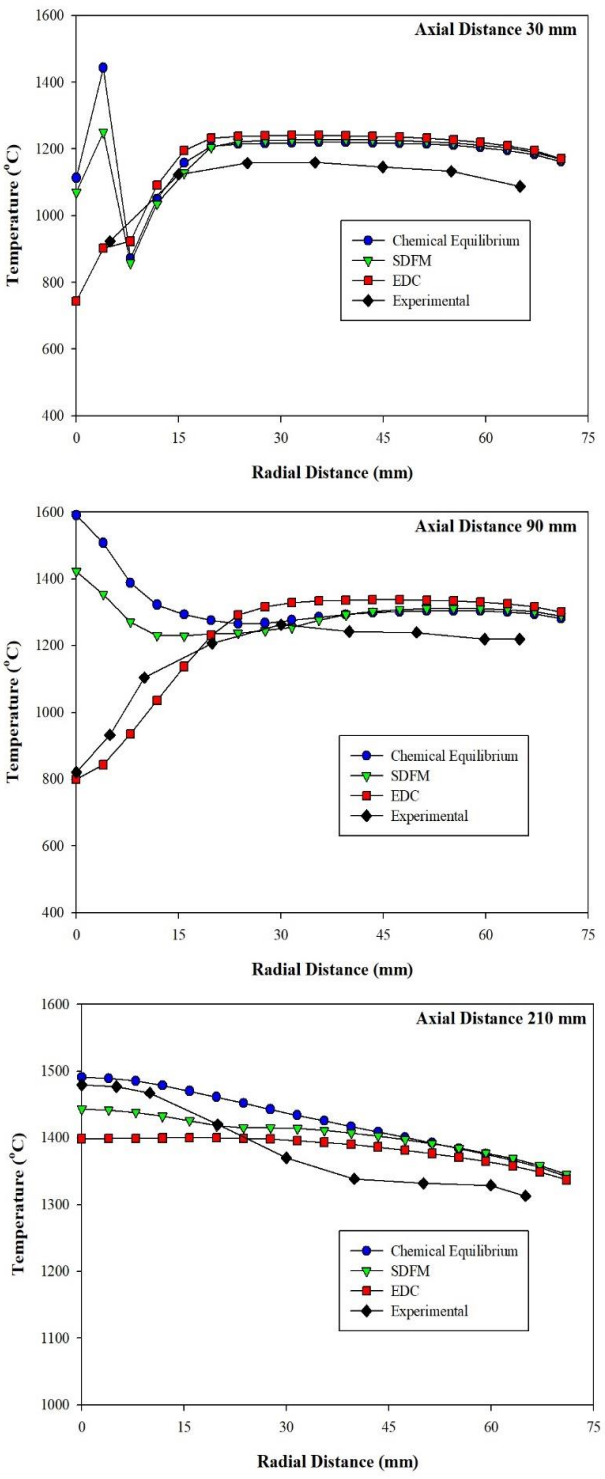

Figure 4. Temperature Comparison for Radial Positions at Different Axial Distances

Hydrogen enrichment studies in the MILD Combustor

The hydrogen enrichment studies were numerically conducted in this paper with two different approaches. The motivation for these studies was the examination of the effects of the hydrogen addition on the combustion mode and fuel reaction rates. The pure methane case in Table 2 was the baseline case (H0) on which the hydrogen enrichment was implemented. The hydrogen addition studies are listed in Table 3. It should be noted that the addition ratios in Table 3 are on molar basis. The inlet temperature of the reactants and wall temperature given in Table 2 were employed for all the cases. In the first series of the numerical analysis, 15.6 kW thermal load and the air excess ratio around 1.6 were kept constant. In the following series, the methane and air consumption rates of the baseline case were kept constant, while the fuel was

enriched with hydrogen on molar basis. Therefore, the thermal load changed between 15.6 kW and 18.72 kW.

Table 3. Hydrogen Enrichment Cases

Constant Thermal Load and Air Excess Ratio		Constant Methane and Air Consumption	
Case	**Fuel**	**Case**	**Fuel**
H0	100% CH_4	H0	100% CH_4
H10 A	90% CH_4 10% H_2	H10 B	90% CH_4 10% H_2
H20 A	80% CH_4 20% H_2	H20 B	80% CH_4 20% H_2
H30 A	70% CH_4 30% H_2	H30 B	70% CH_4 30% H_2
H40 A	60% CH_4 40% H_2	H40 B	60% CH_4 40% H_2

Results

The obtained temperature contours from the numerical analysis are presented in Fig.5 and Fig.6. The constant thermal load and air excess ratio cases are given in Fig.5 and the constant methane and air consumption rate cases are given in Fig.6. It should be noted that the kelvin (K) is the temperature unit in these figures. The maximum temperature of the H0 case is calculated as 1685 K, which proves that the combustion is in the MILD mode. It can be deduced from Fig.5 that the hydrogen enrichment slightly enlarges the flame zone in the combustor. The maximum temperature increases from 1685 K for the H0 case to 1734 K for the H40 A case. It is also seen that the outlet temperature increases with the hydrogen addition. Nevertheless, the general temperature distribution seems to be similar for all the cases. This is due to employing the same thermal load and air excess ratio in all the cases. The one considerable change in the flame temperature distribution by the hydrogen enrichment occurs in the pre-heating zone where the reactants are mixed with the hot products before the combustion takes place. It is seen that this zone is diminished in length as the hydrogen ratio increases. This indicates that the hydrogen addition makes the flame more reactive and the fuel depletion starts over a shorter axial distance from the burner inlet. This can also be commented as the improved flame compactness with the hydrogen enrichment of methane. Fig.6 shows that hydrogen fuel improves the uniformity of the temperature distribution in the combustor. This is due to the additional thermal load stemming from hydrogen having a higher lower-heating value than that of methane. However, the temperature level sets on higher values with the hydrogen addition, which shifts the combustion from the MILD mode to the conventional mode. The maximum temperature rises to 1809 K for the H40 B case from 1685 K for the H0 case. This can also be considered as an effect to favour the NO_X emission formation, which can serve as the basis of future studies. It can also be determined from Fig.6 that the premixing zone in the vicinity of the burner is shortened. This indicates that the hydrogen enrichment alone could increase the methane reactivity even under the constant air and methane consumption conditions.

The variations in the flame parameters with the different hydrogen ratios are given in more details in Fig.7 and Fig.8 for the constant thermal load and air excess ratio condition, and for the constant methane and air consumption condition, respectively. Fig.7 and Fig. 8 present the temperature, OH radical, CH_2O (formaldehyde) and CO variations along the combustor centre, for the cases with 0%, 20% and 40% hydrogen enrichment on molar basis. It can be seen from these two figures that the hydrogen enrichment of methane fuel increases the OH mass fraction in the flame. This increase stems from the two factors. First, hydrogen fuel increases the general flame temperature due to having a higher lower-heating value than that of methane. This contributes to the formation of OH radicals in the flame. Second, decomposition of hydrogen in the flame itself increases the OH radicals. OH radical can be considered as the most reactive radical to deplete CH_4 and H_2 fuels in the flame. Therefore, this shifts the combustion flame upstream to the burner inlet as seen in Fig.7 and Fig.8. The shifting of the combustion flame upstream and increase in the OH mass fraction with the hydrogen enrichment are interlinked. This means that the hydrogen addition to methane makes the combustion flame more reactive and compact. This can also be considered as an effect to depart the flame from the MILD mode to the fast chemistry mode. It can also be deduced that the variations in the flame parameters in Fig.7 and Fig.8 are similar. However, these variations are more distinct for the constant methane and air consumption rate cases given in Fig.8. This is attributed to the higher thermal load and more fuel-rich conditions with the hydrogen enrichment cases in Fig.8. The CH_2O and CO mass fractions also show a similar variation trend with the other flame parameters. These two species are shifted upstream with the increasing hydrogen ratio. It can be seen that the maximum values of the CH_2O and CO mass fractions increase and their distribution ranges are narrowed with the increasing hydrogen ratio. The results from the CH_2O and CO variations, as the intermediate species, indicate that the reactions occur more intensely in a narrower zone in the flame with the hydrogen enrichment, which diminishes the MILD behaviour of the combustion. As the hydrogen addition ratio increases from 0% to 40%, the calculated CO level in the exhaust gas decreases from 18 PPM to 13 PPM on dry basis for the constant thermal load and air excess ratio condition. This is generally due to the increased OH mass fraction and reduced carbon-containing species in the flame. In contrast, it is increased from 18 PPM to 35 PPM on dry basis for the constant methane and air consumption condition. This arises from the fact that the air consumption rate is kept constant and this shifts the flame to a more fuel-rich condition with the hydrogen addition.

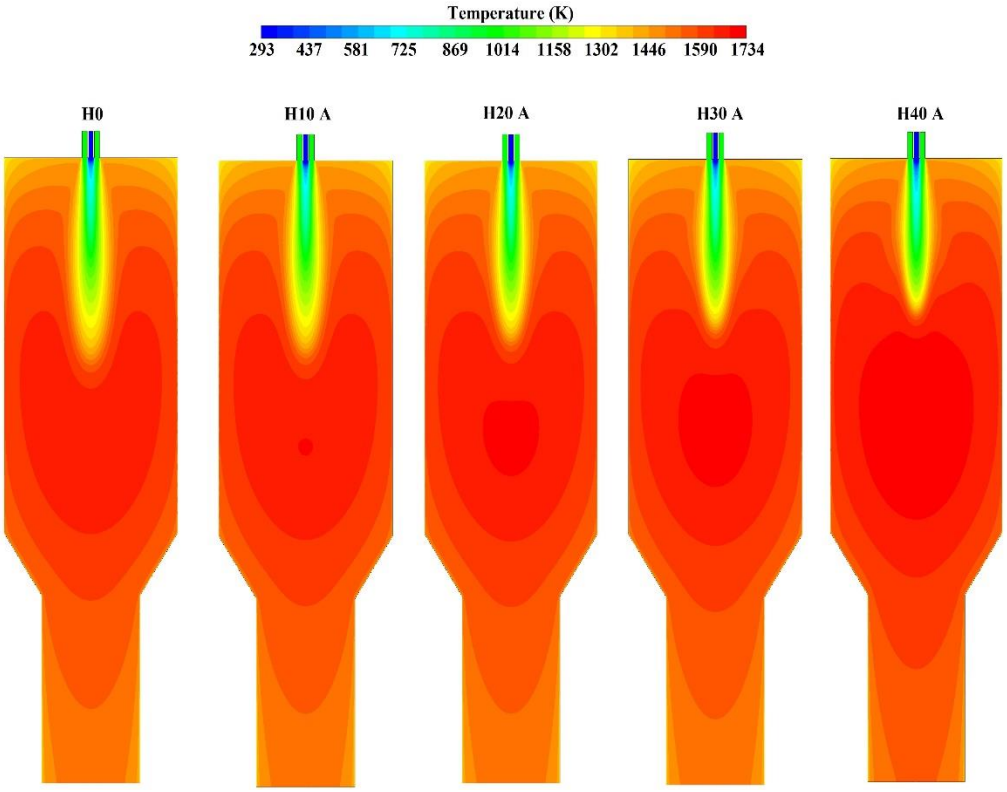

Figure 5. Temperature Contours for Constant Thermal Load and Air Excess Ratio

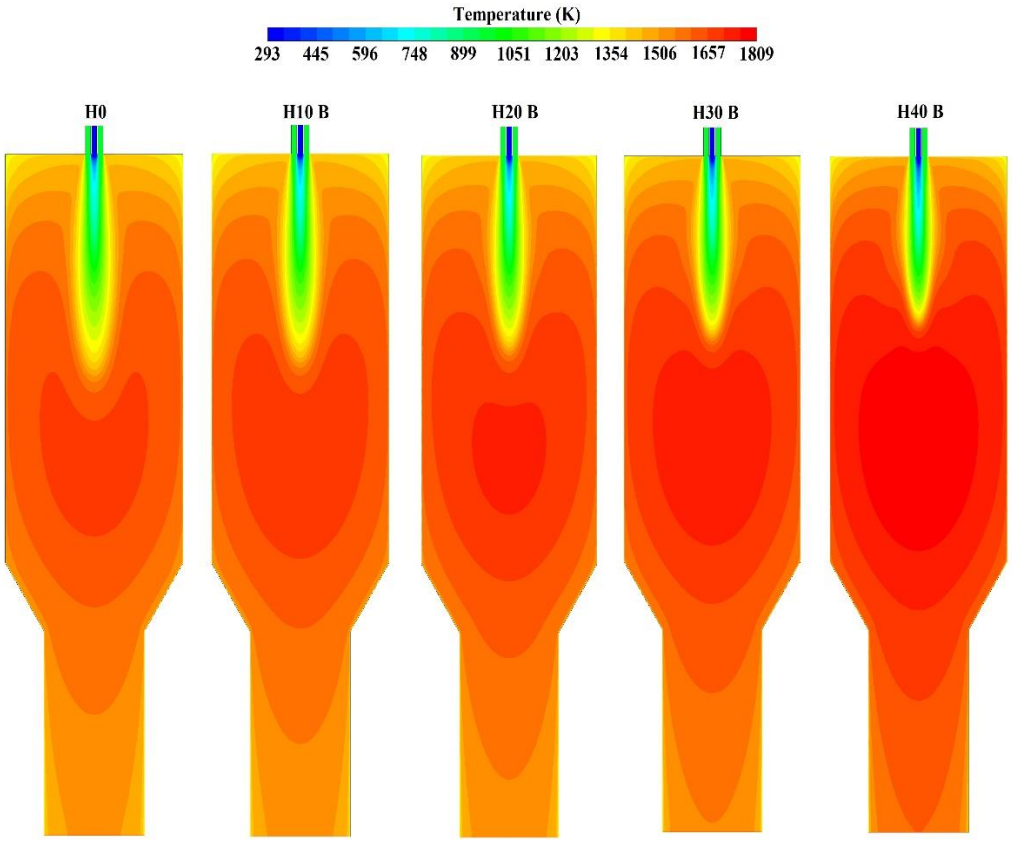

Figure 6. Temperature Contours for Constant Methane and Air Consumption Rate

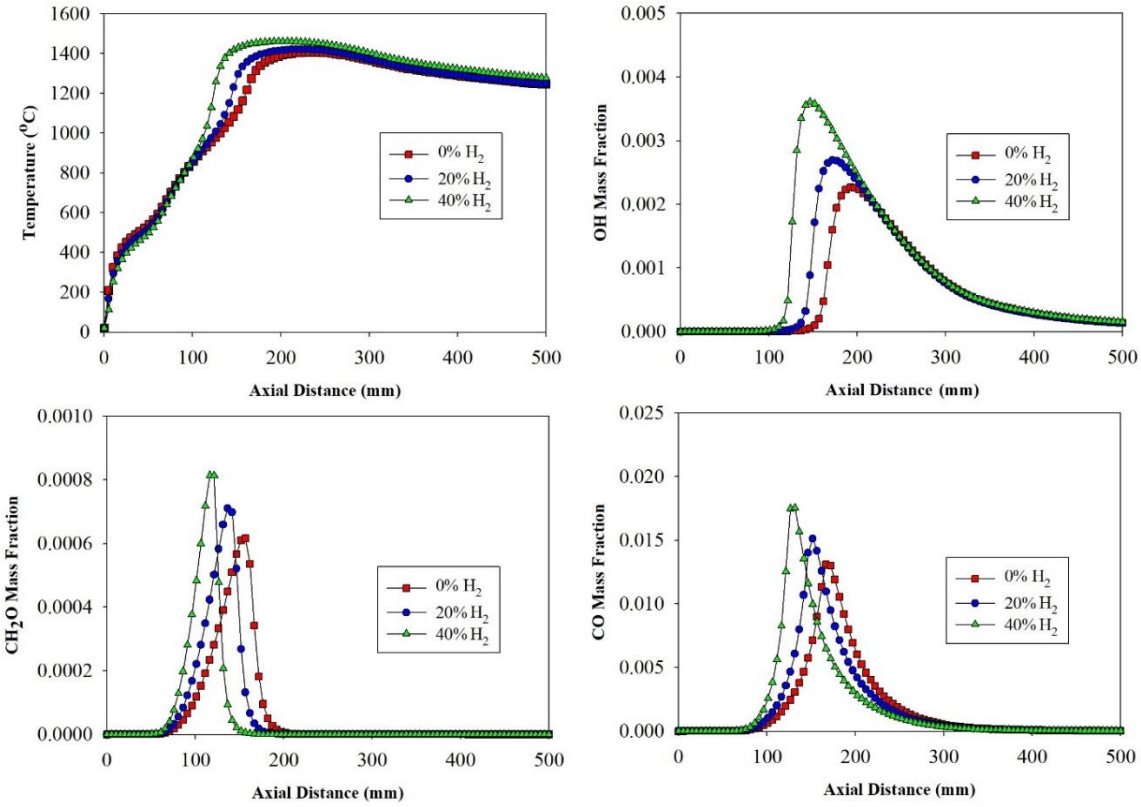

Figure 7. Flame Parameters along Combustor Centreline for Constant Thermal Load and Air Excess Ratio

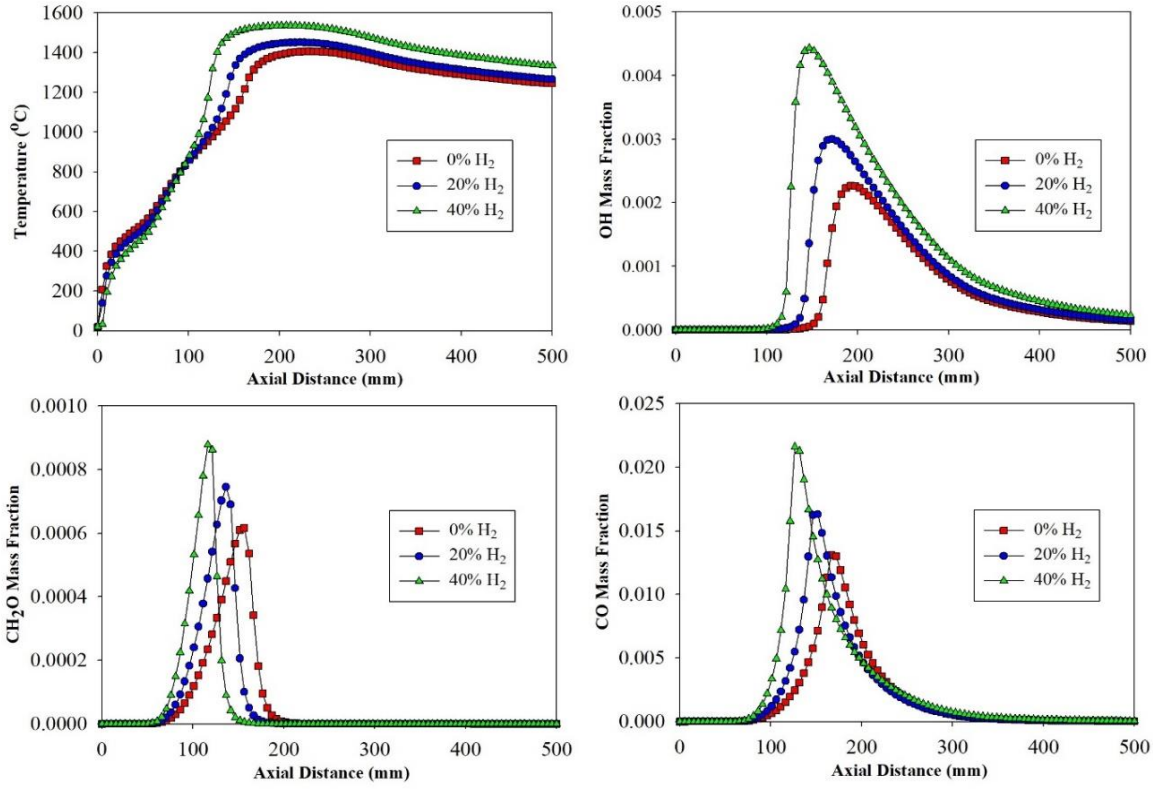

Figure 8. Flame Parameters along Combustor Centreline for Constant Methane and Air Consumption Rate

The local reaction rates of CH_4 along the combustor centre are presented in Fig.9 for the constant thermal load and air excess ratio cases, and for the constant methane and air consumption rate cases. The calculated results show that the hydrogen enrichment increases the depletion rate of CH_4 fuel, making it more reactive. The maximum reaction rate point is shifted upstream with the hydrogen addition to methane. This indicates that the CH_4 fuel is reacted over a shorter axial distance from the burner inlet limiting its dissipation into the radial zones. These results from the reaction rate of CH_4 are consistent with the temperature and chemical species distributions given in Fig.7 and Fig.8. The reaction rate variations with the hydrogen addition are more distinct for the cases with the constant methane and air consumption rate. This is due to higher flame temperature and CH_4 concentration in the reaction zone. The most significant result from Fig.7, Fig.8 and Fig.9 is that the hydrogen addition alone increases the reaction rate of CH_4 and influences the combustion mode even for the constant methane and air consumption scenarios.

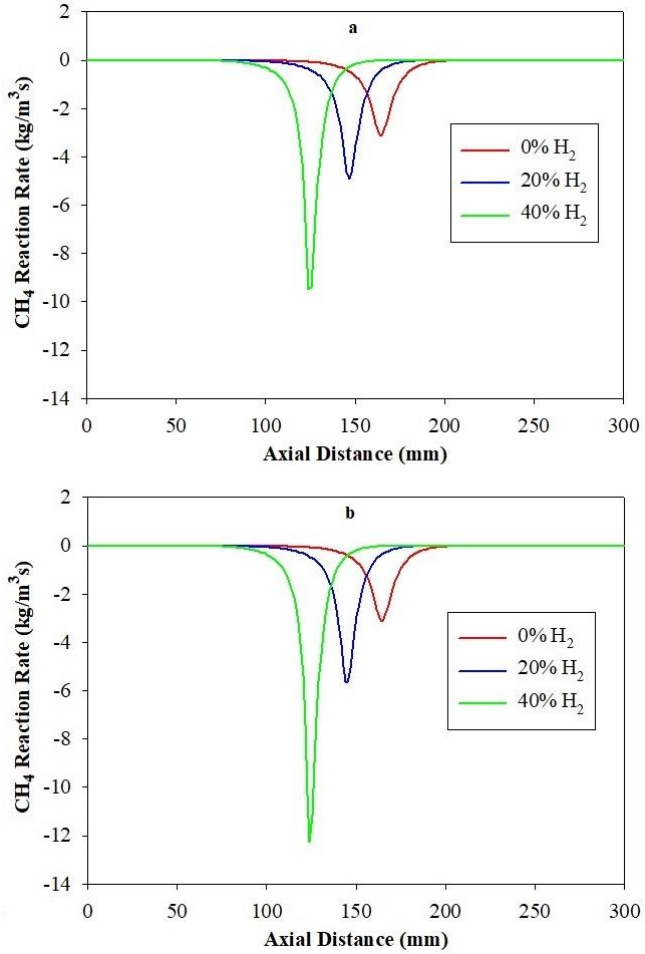

Figure 9. Calculated Reaction Rates of CH_4 along Combustor Centreline for the Constant Thermal Load and Air Excess Ratio Cases (a) and for the Constant Methane and Air Consumption Rate Cases (b)

An additional study was conducted on the flow field alteration by the hydrogen enrichment of methane fuel. The recirculation ratio of the combustion products at any axial location was calculated using Eq. (10). This equation was derived based on the fact that the mass flow rate in the combustor at any axial location equals to the inlet rate of the reactants. The integral in the equation is equal to the sum of the inlet rate of the reactants and twice the recirculated mass flow rate, since the absolute value of the axial velocity is taken into account. Eq. (10) was solved over the converged simulation results and the integrations were numerically performed in the simulation software. The calculated velocity iso-surfaces for the pure methane case (H0) and the recirculation ratio results from the solution of Eq. (10) are given in Fig.10.

$$\frac{0.5 \text{ x } (\int_0^{R_c} \rho |u_x| \, 2\pi r \, dr - \dot{m}_{fuel} - \dot{m}_{air})}{\dot{m}_{fuel} + \dot{m}_{air}} \quad (10)$$

Fig.10a shows the recirculation zones close to the burner walls that form due to the convergent nozzle placed in the end of the combustor. The MILD combustion mode in this combustor is dependent on this recirculation of the hot combustion products into the reactants. Fig. 10b and 10c show that the recirculation rate at any axial location is diminished with the hydrogen enrichment of methane. This is another effect of hydrogen, which diminishes the MILD combustion mode in the combustor. This effect is seen to be more influential for the cases with the constant methane and air consumption rate. The reduction in the recirculation ratio is due to the decreased axial momentum of the combustion air and increased axial momentum of the fuel jet for the constant thermal load and air excess ratio cases. The reduction stems from the increased axial momentum of the fuel jet only for the constant methane and air consumption rate cases. The effects of the temperature and reaction intensity variations on the flow field alteration can also be the focus of future studies.

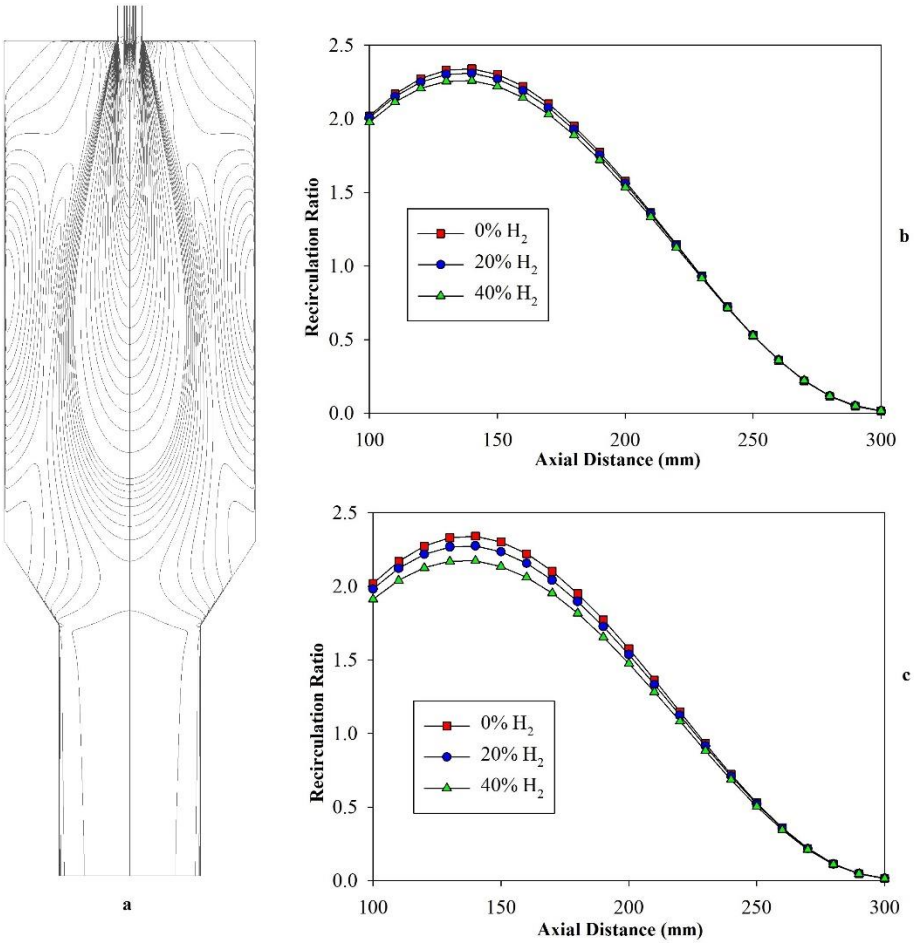

Figure 10. Velocity Iso-Surfaces for Pure Methane Case (a), Recirculation Ratio for the Constant Thermal Load and Air Excess Ratio Cases (b) and the Constant Methane and Air Consumption Rate Cases (c)

Conclusion

This study examines on the hydrogen-enriched methane combustion characteristics in a MILD combustor. The hydrogen addition ratio changes from 10% to 40% on molar basis for the two scenarios, namely the constant thermal load and air excess ratio cases and the constant methane and air consumption cases. The conclusions from this study are as follows;

- EDC combustion model performs the best to predict the experimental measurements in the flame. This means that the combustion is not fully in the mixed-controlled mode and the finite-rate kinetics influences the general reaction rates.

- The MILD methane combustion case has a maximum temperature of 1685 K. This temperature value increases to 1734 K for the constant thermal load and air excess ratio case with 40% hydrogen enrichment. In addition, the maximum temperature increases to 1809 K for the constant methane and air consumption case with 40% hydrogen enrichment. The difference in the temperature increment is due to the shifting of the flame to more fuel-rich conditions.

- The hydrogen addition to methane shifts the flame upstream to the burner inlet zone. This is mainly caused by the increase in the OH fractions, which ultimately increases the general reaction intensity in the flame. Therefore, the main intermediate species, CO and CH_2O, are also shifted upstream and their maximum values are also increased. These variations indicate that the flame diminishes its MILD behaviour with the hydrogen enrichment. It should be stated that the NO_x emission formation is expected to increase with hydrogen addition due to the flame temperature rise, which can be the focus of future studies.

- The hydrogen enrichment of methane fuel reduces the recirculation ratio in the combustor with the convergent nozzle exit. This clearly indicates that the hydrogen addition reduces the MILD behaviour of the flame, since the MILD mode for this combustor is dependent on the recirculation

of the hot combustion products into the reactants. The reduction in the recirculation ratio is mainly due to the increased axial momentum of the fuel jet, when methane fuel is enriched with hydrogen.

Ethics Committee Approval and Conflict of Interest Statement

There is no need to obtain permission from the ethics committee for the article prepared.

There is no conflict of interest with any person / institution in the article prepared.

Acknowledgement

Not applicable.

Nomenclature

c_p Mixture specific heat (kJ/kg K)

D Diffusion coefficient (m^2/s)

f Mixture fraction

f_i Force acting on i_{th} species (N/kg)

$\bar{f}$ Mean mixture fraction

$\overline{f'^2}$ Mean mixture fraction variance

$\bar{H}$ Mean enthalpy level (kJ/kg)

h Total enthalpy (kJ/kg)

J_i Diffusion flux of i_{th} species (kg/m^2s)

k_L Thermal conductivity coefficient (kW/m K)

Le Lewis Number

$\dot{m}$ Mass flow rate (kg/s)

P Stress Tensor (N/m^2)

R_i Reaction rate of i_{th} species (kg/m^3s)

R_c Combustor radius (m)

Sc_t Turbulent Schmidt number

S_h Source term for radiation (kJ/m^3s)

T Temperature (K)

t Time (s)

u_x Axial velocity (m/s)

v Velocity vector (m/s)

Y_i Mass fraction of i_{th} species

μ_t Turbulent viscosity (kg/m s)

ξ^* Length fraction of fine scales

ρ Density (kg/m^3)

τ^* Time scale (s)

$\emptyset$ Scalar term

χ_{st} Stoichiometric scalar dissipation rate (s^{-1})

σ_t Model constant

Abbreviations

EDC Eddy dissipation concept

MILD Moderate or intense low-oxygen dilution

PPM Parts per million

SDFM Steady diffusion flamelet model

References

[1] A. Cavaliere and M. de Joannon, "MILD combustion," Progress in Energy and Combustion Science, vol. 30, no. 4, pp. 329-366, Apr. 2004.

[2] C. Luan, S. Xu, B. Shi, Y. Tu, H. Liu, P. Li and Z. Liu, "Re-Recognition of the MILD combustion regime by initial conditions of T_{in} and X_{O2} for methane in a nonadiabatic well-stirred reactor," Energy&Fuels, vol. 34, no. 2, pp. 2391-2404, Jan. 2020.

[3] J.A. Wünning and J.G. Wünning, "Flameless oxidation to reduce thermal NO-formation," Prog. Energy Combust. Sci., vol. 23, no. 1, pp. 81-94, 1997.

[4] A. Rimkus, "Effect of hydrogen addition on the energy and environmental performance of a compression ignition dual-biofuel engine," International Journal of Hydrogen Energy, vol. 217, 153709, Mar. 2026.

[5] A.G.H. Saif and E.M.A. Mokheimer, "Comprehensive review on ammonia combustion technologies: combustion characteristics, potential of hydrogen/methane additions, and emerging applications," International Journal of Hydrogen Energy, vol. 148, 149672, Jul. 2025.

[6] A. Rebola, M. Costa and P.J. Coelho, "Experimental evaluation of the performance of a flameless combustor," Applied Thermal Engineering, vol. 50, no. 1, pp. 805-815, Jan. 2013.

[7] E.E. Fordoei, K. Mazaheri and A. Mohammadpour, "Numerical study on the heat transfer characteristics, flame structure, and pollutants emission in the MILD methane-air, oxygen-enriched and oxy-methane combustion," Energy, vol. 218, 119524, Mar. 2021.

[8] A. Rebola, P.J. Coelho and M. Costa, "Assessment of the performance of several turbulence and combustion models in the numerical simulation of a flameless combustor," Combustion Science and Technology, vol. 185, no. 4, pp. 600–626, Mar. 2013.

[9] E.S. Rashed, A.E. Elwardany, M. Emam, S.A. Elfadl, S. Mori and H. Hassan, "3D numerical study of NH_3/H_2 MILD combustion in a reversed flow MILD combustion furnace," Applied Thermal Engineering, vol. 252, 123610, Sep. 2024.

[10] S. Xu, Z. Tian, Y. Chen, S. Liang, Y. Tu and H Liu, "Effect of hydrogen-blending ratio and wall temperature on establishment, NO formation, and heat transfer of hydrogen-enriched methane MILD combustion," Fuel, vol. 369, 131787, Aug. 2024.

[11] M. Zourazmai, M.Z. Targhi and A. Ashouri, "Enhancing temperature uniformity and recirculation in MILD combustion furnace: a study on angle of burner's bluff body," Case Studies in Thermal Engineering, vol. 73, 106561, Sep. 2025.

[12] S. Jowkar, L. Deng and X. Shen, "Numerical assessment of ammonia spray combustion in a swirl burner under MILD conditions for clean and low-NOx operation," Applied Thermal Engineering, vol. 282, 128858, Jan. 2026.

[13] A. Mardani, H. Kim, S. Oh, K.C. Kim, X. Xia and F. Qi, "Experimental investigation of an ammonia-hydrogen-methane non-premixed high swirl model combustor for preheated and diluted air regime," International Journal of Hydrogen Energy, vol. 207, 153430, Feb. 2026.

[14] M.K. Büyükakın, "Effects of hydrogen addition on methane fuel reactivity in high-temperature $CO_2/O_2/N_2$ coflow in a non-premixed lab-scale tube burner," International Journal of Hydrogen Energy, vol. 206, 153377, Feb. 2026.

[15] C.K. Law, "Conservation equations," in Combustion Physics, Cambridge University Press, New York, 2006, pp. 157-193.

[16] ANSYS Fluent Theory Guide, 2021, https://dl.cfdexperts.net/cfd_resources/Ansys_Documentation/Fluent/Ansys_Fluent_Theory_Guide.pdf, Accessed 21 Sep. 2025.

[17] A. Kazakov and M. Frenklach, "Reduced reaction sets based on GRI-Mech 1.2," http://combustion.berkeley.edu/drm/, Accessed 06 Apr. 2026.